Carbohydrate Polymer Technologies and Applications 2 (2021) 100121

Contents lists available at ScienceDirect

Carbohydrate Polymer Technologies and Applications

journal homepage: www.sciencedirect.com/journal/carbohydrate-polymer-technologies-and-applications

Nanostarch production by enzymatic hydrolysis of cereal and tuber starches

Ajinath S Dukare [a,b], A. Arputharaj [b], A.K. Bharimalla [b], Suajata Saxena [b], N. Vigneshwaran [b,*]

[a] ICAR-Central Institute of Post-Harvest Engineering & Technology, Abohar 152116, Punjab India
[b] ICAR-Central Institute for Research on Cotton Technology, Mumbai 400019, Maharashtra India

ARTICLE INFO

Keywords:
Acid hydrolysis
α-Amylase
Crystallinity
Nanostarch, Scanning electron microscopy (SEM)
Transmission electron microscopy

ABSTRACT

In this work, nanostarch was extracted from cereal (maize) and tuber (potato and cassava) crops by an enzymatic process and characterized. Simultaneously, the conventional acid hydrolysis process was carried out to produce nanostarch. These nanostarches were characterized by different techniques such as dynamic light scattering (DLS), fourier-transform infrared (FTIR) spectroscopy, X-ray diffraction (XRD), differential scanning calorimetry (DSC), scanning electron microscopy (SEM) and transmission electron microscopy (TEM). The smallest size was achieved in the case of maize starch, 18 ± 3 nm by acid hydrolysis and 162 ± 23 nm by the enzyme hydrolysis. The nanostarch yields by enzymatic process were 18, 29 and 41 wt% for maize, potato and cassava starches, respectively. Significant reduction in the crystalline region of starch was observed after enzyme hydrolysis, as analyzed by relative crystallinity using XRD spectra. The reduction of amorphous region in nanostarch decreased its melting enthalpy as demonstrated by DSC. Enzyme hydrolyzed nanostarch could find its potential application as fillers not only for their reinforcing properties in biocomposites but also for its renewability and biodegradability.

1. Introduction

Starch is a naturally occurring most abundant, renewable, and biodegradable polysaccharide that is synthesized and stored as a source of energy by most of the plants. Nevertheless, the application of native starch is often restricted owing to its constricted solubility, weak functional attributes, and limited tolerance to a wide array of processing conditions (Yu et al., 2021). On the contrary, starch-based nanoparticles are gaining more attention due to their improved suspending property, bio-accessibility, and controllable release behavior. Consequently, starch nanoparticles find applications in diverse areas, including drug delivery systems, biocomposites, emulsion stabilizers, hydrogel, aerogel, bioplastics, and paper products (Dong et al., 2021). Additionally, physical and chemical modifications of starch could facilitate the production of diverse commodity chemicals (Roy Goswami et al., 2016). The latest fine chemical extracted from starch in the 21stcentury is nanostarch, having one or more dimensions in the nanoscale region. Due to the increased surface area and modified crystalline and other properties, nanostarch finds potential applications in bionanocomposites, pharmaceuticals, and food/feed products. Many reviews are available towards the methods for extraction and preparation of nanostarch, chemical modifications, reinforcing effects and mechanisms, and their potential applications (Lin, Huang, Chang, & Anderson, 2011; Le Corre et al., 2010; Kim et al., 2015; Le Corre & Angellier-Coussy, 2014).

In contrary to the native starch, starch nanoparticles have more surface area and modified amorphous/crystallinity ratio. During the last few decades, manifold techniques have been used for the preparation of nano-sized particles from the starch biopolymer. Nanostarches are mainly synthesized by “top-down” (e.g., acid hydrolysis, enzyme hydrolysis or physical treatments) and “bottom-up” approaches (e.g., self-assembly and nanoprecipitation). The conventional method of nanostarch synthesis is sulfuric acid hydrolysis followed by ultrasonic treatment (Rajisha et al., 2014). More recently, researchers have attempted to prepare nanostarch from native starch by acid hydrolysis (Putro et al., 2020), homogenization (Apostolidis & Mandala, 2020), rapid ultrasonication (Chang et al., 2019), microemulsion (Qi et al., 2017), rapid antisolvent nanoprecipitation (Dong et al., 2021), ionic gelation (Liu et al., 2020), alkali freezing and cross-linking (Xiao et al., 2020), acid hydrolysis and ultrasound technique (Shabana et al., 2019) and enzyme-based approach (Cuthbert et al., 2017).

Highly dispersed palladium-nanoparticles grafted onto amino-functionalized nanostarch were demonstrated to be excellent heterogeneous catalysts for direct conversion of various aromatic iodides to their corresponding aldehydes in excellent yields without using any

* Corresponding author.
E-mail address: Vigneshwaran.N@icar.gov.in (N. Vigneshwaran).

https://doi.org/10.1016/j.carpta.2021.100121
Received 30 April 2021; Received in revised form 30 June 2021; Accepted 11 July 2021
Available online 14 July 2021
2666-8939/© 2021 The Author(s). Published by Elsevier Ltd. This is an open access article under the CC BY-NC-ND license (http://creativecommons.org/licenses/by-nc-nd/4.0/).

base. The developed catalyst was recovered and recycled several runs without any significant loss in its activity (Kumar et al., 2015). Nanostarch was also used for grafting of oxo-vanadium Schiff base catalyst for use in the oxidation of alcohols (Verma et al., 2013). The nanostarch derived from tapioca starch was highly effective in filtration control in water-based drilling muds (Zoveidavianpoor & Samsuri, 2016). The nanostarch was demonstrated as a carrier for diclofenac sodium drug for enhancing its controlled release and successful permeation, thus, offering a promising nano-system for the transdermal delivery of a non-steroidal anti-inflammatory drug (El-Naggar et al., 2015). The reinforcing effects of nanostarch have been demonstrated as excellent nanofiller for natural rubber latex and have the potential for replacing conventional fillers like carbon black and silica, which are a real threat to the environment (Rajisha et al., 2014). The starch nanoparticles prepared by using *in situ* nanoprecipitation and water-in-oil microemulsion methods were efficiently used to load the curcumin for its controlled release (Acevedo-Guevara et al., 2018; Chin et al., 2014). As demonstrated in amaranths protein based composite film, the nanostarch may also improve the mechanical and barrier properties of the composite film (Condés et al., 2015). The state-of-the-art in the field of starch-based nano-biocomposites was reviewed in the year 2013 (Xie et al., 2013). In other applications, starch nanoparticles prepared using non-solvent precipitation could be used in pickering emulsions (Fuentes, Sjöö, Rayner, &Wahlgren, 2017). Most of these nanostarch preparing methods have some concerns, such as the use of toxic chemicals and very high energy cost economics. Consequently, there is a growing interest to develop more greener and eco-friendly processes for processing the starch biopolymer (Maleki et al., 2019; Maleki et al., 2017). A newer scalable physical method of starch nanoparticle production by stirred media milling reduced the original particle size of native starch from 3–20 μm to around 245 nm in 90 min (Patel et al., 2016). But, nanostarch synthesized by this method had low stability of less than a week. Some researchers have also tried to prepare nanostarch using an enzymatic process, which is a greener and eco-friendly method. Using enzyme-catalyzed hydrolysis, the synthesis of spherical or oval-shaped nanostarch with a significant loss due to hydrolysis (85 to 90%) was also reported (Kim & Lim, 2009). Likewise, nanostarch was prepared from the *Proso* millet by enzymolysis and recrystallization wherein the yield was about 55% (Sun et al., 2014).

Several enzymes obtained from diverse microorganisms have been extensively used in many foods and non-food sectors. Worldwide, the diverse roles of amylases extracted from fungal and bacterial sources in different areas are well recognized and have been reported by various researchers. In this context, as a replacement for the conventional acid hydrolysis process, microbial amylases can be used in the controlled hydrolysis of starch granules to produce nano-sized particles from the native starch. Maize, cassava, wheat, and potato are the major sources for starch production and they are either used by industry as such or after modification (Waterschoot et al., 2015). With this background, herein, we have prepared the nanostarch from maize, potato, and cassava starch by enzymatic (α-amylase) and acid hydrolysis processes. Further produced nanostarches have been characterized by various techniques.

2. Materials and methods

2.1. Materials

Three different starches were used for the preparation of nanostarch, *viz.*, one cereal starch (maize) and two tuber starches (potato and cassava). All the types of starch were of analytical grade, purchased from Sigma Aldrich. The amylase enzyme used is BAN® 480L (Novozymes), α-amylase produced by submerged fermentation of a selected strain of *Bacillus amyloliquefaciens*. The systematic name is 1,4-alpha-D-glucan glucano-hydrolase (EC 3.2.1.1).

2.2. Proximate analysis of starch

Moisture, protein, and ash content were determined using standard methods (AOAC, 2005). The lipid/oil content was determined using standard methods (AOAC, 2005). The total amount of soluble sugars was determined using 0.5 g starch after extraction using ethanol (95%) and subsequent quantification using the method given by DuBois et al., and Smith (1956). The crude fiber was determined according to a method described earlier (Repo-Carrasco-Valencia et al., 2009).

2.3. Nanostarch production

The conventional acid hydrolysis process of nanostarch preparation was carried out as described earlier (Angellier et al., 2004). Briefly, 44.1g starch was suspended in 300 mL of 3.16 M sulfuric acid solution in a 1000 mL Erlenmeyer flask and incubated at 40 ± 0.2°C in a reciprocal shaker for five days at 100 rpm. After 5 days, the starch suspension made acid free by successive centrifugation in deionized water at 10,000 rpm for 10 min, till achieving the neutral pH. The final starch pellet was suspended in 300 mL deionized water and characterized further.

For the enzymatic process, 1 g starch was suspended in 100 mL deionized water and incubated at 60 ± 0.2°C on a reciprocal shaker with the α-amylase enzyme at a concentration of 0.1 U/g of starch for 30 min. After completion of the incubation period, the reaction mixture was centrifuged at 10,000 rpm for 10 min and re-suspended in deionized water and used for further analysis. The supernatants that contained the enzyme and soluble sugars were discarded. The nanostarch was freeze dried for FTIR and XRD analyses. The yield of nanostarch was calculated based on the weight of the freeze dried powder obtained.

2.4. DLS Particle size analysis

The average particle size was measured using the Nicomp™ 380 ZLS analyzer. Size calibration was carried out using 90 nm size polystyrene latex spheres. The size distribution was obtained based on the dynamic light scattering (DLS) and autocorrelation principle. The mean diameter of the particles was calculated from their Brownian motion via the Stokes–Einstein equation. For this, a He–Ne laser (632.8 nm) was used and scattering intensity was analyzed by Avalanche photodiode detector at 90° orientation.

2.5. Scanning electron microscopy

The morphology of nanostarch was observed in a scanning electron microscope (Philips, XL 30 SEM). A drop of liquid nanostarch aqueous suspension was added on a sample holder (SEM stub) and dried under an IR lamp and samples were transferred to a sputter coater for gold / palladium coating. After uniform coating of a conductive layer, the samples were observed under the SEM at an accelerating voltage of 12 kV.

2.6. Transmission electron microscopy

For TEM analysis, a drop of dilute aqueous solution containing the nanostarch (0.1%) was placed on the carbon-coated copper grids and dried at room temperature. The micrographs were obtained using Philips® EM208 operating at 200 kV. Uranyl acetate was used to enhance the contrast. Simultaneously, selected area electron diffraction (SAED) patterns were recorded for all the samples. ImageJ® software was used for size analysis from the TEM micrographs. For this, the TEM micrographs were first converted to 8-bit images. The scale bar in the micrograph was used to calibrate the software. Then, the threshold adjustment was done followed by drawing the outlines of the particles by adjusting the image contrast. Finally, the particle size analysis was done and reported.

Table 1
Proximate analysis of starches from maize, potato and cassava.

Starch	Moisture content (%)	Reducing sugar content	Ash (%)	Protein (%)	Crude fibre (%)	Total fat (%)
Maize	11.80	0.44	0.50	2.80	2.44	0.31
Potato	12.50	0.35	0.29	1.33	0.28	0.77
Cassava	15.20	0.32	0.33	0.68	0.41	0.56

2.7. X-ray diffraction analysis

Wide angle X-ray diffraction patterns of native starch and nanostarch (freeze dried) were obtained using a Philips®PW1710 X-ray diffractometer with nickel filtered Cu Kα(λ= 1.54Å) radiation and analyzed using automatic powder diffraction (APD) software. The diffracted intensities were recorded from 10° to 80°2θangles. The relative crystallinity of the starch was calculated using the formula, Ac/(Aa + Ac), where Ac was the crystalline area, and Aa was the amorphous area on the XRD spectra.

2.8. Fourier transform infrared spectroscopy analysis

For FTIR analysis, the freeze dried nanostarch was diluted with potassium bromide in the ratio of 1:100 and made into a pellet. This pellet was analyzed using an IRPrestige-21® FTIR in transmission mode, with a resolution of 4 cm^{-1}. The spectra recorded were the average of 64 scans and the contribution of the background was accounted for during analysis.

2.9. DSC analysis

The thermal transition properties of nanostarch were examined using a differential scanning calorimeter (Mettler®) in nitrogen atmosphere. The instrument was calibrated with indium and an empty pan was used as the reference. The starch sample (3.0 mg, dry basis) and water (6.0 mg) were transferred to an aluminum DSC pan, which was then hermetically sealed and equilibrated at 4°C for 2 h before analysis. The sample pan was scanned from 40°C to 180°C at a heating rate of 5°C/min.

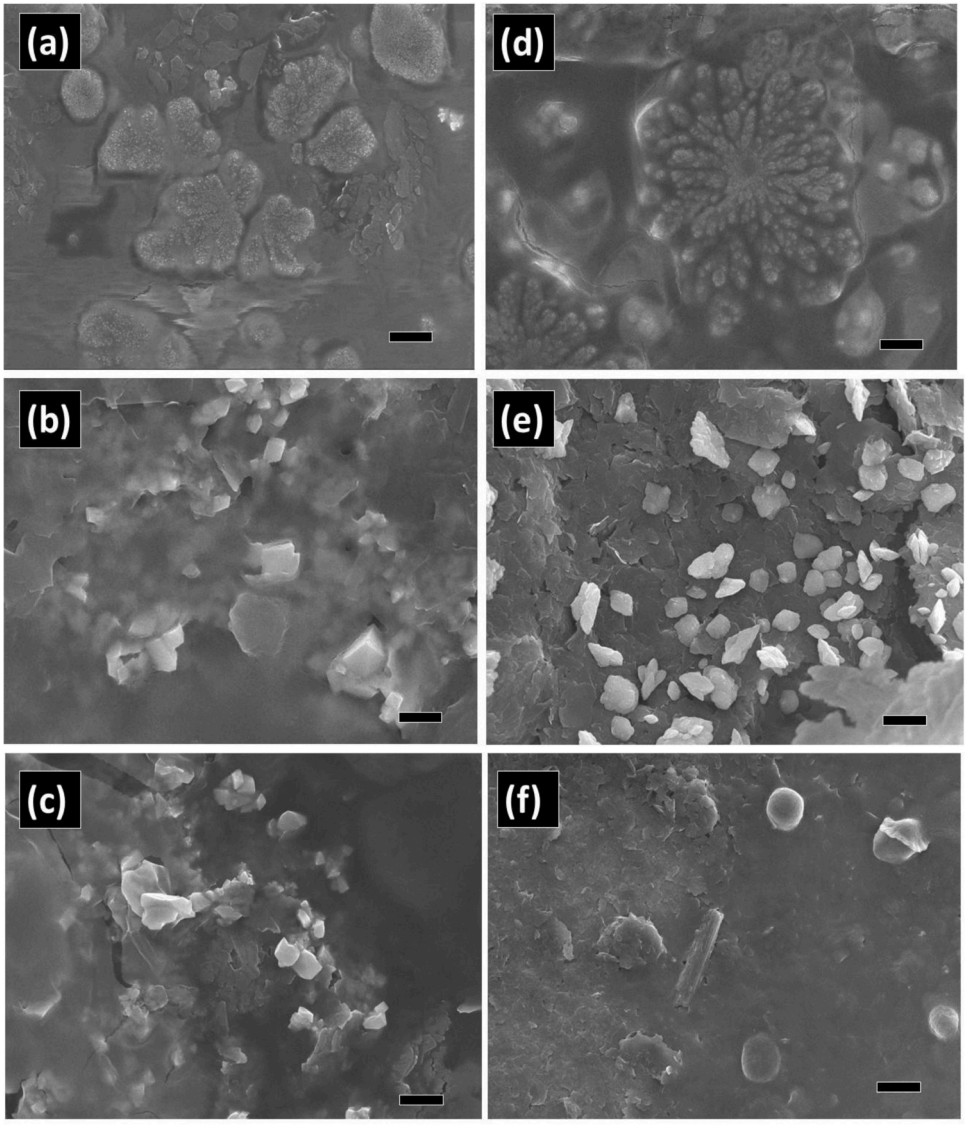

Fig. 1. SEM images of acid hydrolyzed nanostarch from maize (a), potato (b) and cassava (c) and enzyme hydrolyzed nanostarch from maize (d), potato (e) and cassava (f). Scale bars correspond to 1 μm.

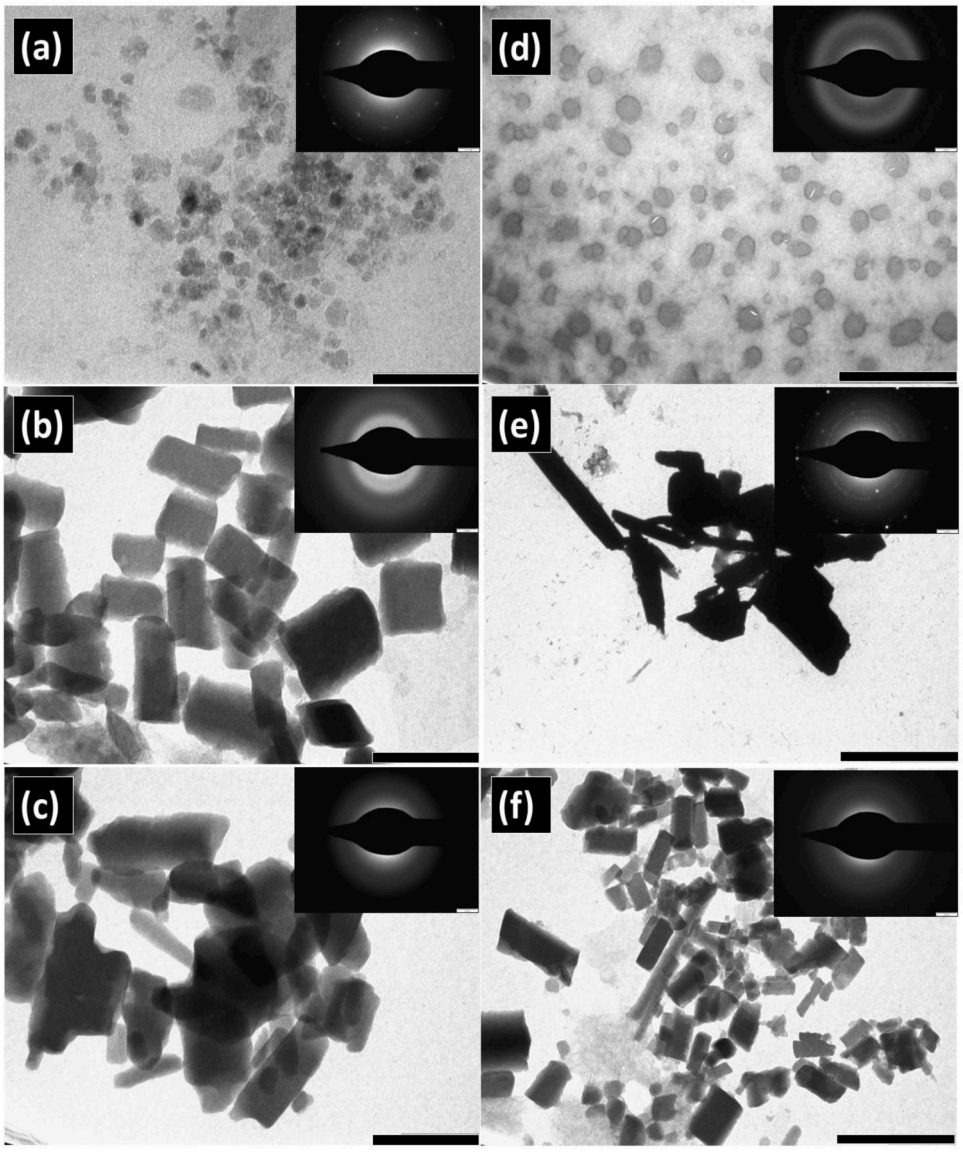

Fig. 2. TEM images of acid hydrolyzed nanostarch from maize (a), potato (b) and cassava (c) and enzyme hydrolyzed nanostarch from maize (d), potato (e) and cassava (f). Scale bars correspond to 100 nm for a, b and c and 1 μm for d, e and f.

Table 2
Size distribution of nanostarches as evaluated by dynamic light scattering (DLS) and transmission electron microscopy (TEM). All the values are mean of 3 replications ± SE.

Sources of nanostarch	Size by DLS		Size by TEM	
	Acid hydrolysis	Enzyme hydrolysis	Acid hydrolysis	Enzyme hydrolysis
Maize	18 ± 3 nm	162 ± 23 nm	22 ± 5 nm	140 ± 40 nm
Potato	78 ± 17 nm	301 ± 90 nm	55 ± 14 nm	275 ± 120 nm
Cassava	88 ± 24 nm	255 ± 61 nm	72 ± 29 nm	210 ± 80 nm

3. Results and discussion

Starch is an abundant, natural, renewable and biodegradable polymer produced by many plants as a source of stored energy. Due to the structure of starch granules consisting of alternating crystalline and amorphous concentric layers, the controlled acid hydrolysis treatment of native starch disrupts this organization and releases crystalline platelet-like particles with nanoscale dimensions (Dufresne, 2015). The dimensions of native starch granules are critical for controlling digestion by amylase. In general, small starch granules are digested faster than large granules due to their larger exposed surface area (Qi & Tester, 2016). The average sizes of maize, potato and cassava starch granules were 16.9 μm, 50.4 μm and 16.3 μm, respectively (Md. Sharif et al., 2011). The proximate analysis of starches from maize, potato and cassava is given in Table 1. The moisture content was highest in the cassava starch followed by potato starch and maize starch. The ash content was highest in maize starch followed by cassava and potato. Additionally, protein and fat were also present in a significant amount.

In this work, enzyme hydrolysis yielded 18, 29 and 41 wt% of nanostarch for maize, potato and cassava starches, respectively. In case of acid hydrolysis, it was 16, 25 and 35 wt%, respectively for maize, potato and cassava starches. Here, apart from the initial granular sizes of starches, their internal structure might have played a role in deciding the final yield of the nanostarch; but the yield trend looked similar in both the enzymatic and acid hydrolyses for all three types of starch. In an earlier report, it was possible to obtain starch nanocrystals after only 5 days of sulfuric acid hydrolysis with a yield of 15 wt % and having the same shape as those obtained from the classical procedure after 40 days of HCl treatment, with a yield of 0.5 wt % (Angellier et al., 2004). In this

Table 3
Examples of recent studies reporting the enzymatic preparation of nanostarches and their relevant characteristics.

Sources of starch	Preparation method	Shape	Size (nm)	References
Waxy potato starch	Enzymatic (glucoamylase) pretreatment by sulfate acid hydrolysis	Square	50 to 100	(Hao, Chen, Li, & Gao, 2018)
Waxy maize starch	Enzymatic treatment with pullulanase.	Globular	5 to 25	(Chena Aldao et al., 2018)
Teff starch	Enzymolysis	Irregular	3 to 10	(Cuthbert, Ray, & Emmambux, 2017)
Maize starch	Enzymolysis	Irregular	2.4 to 6.7	(Cuthbert et al., 2017)
Maize starch	Enzymolysis (Pullulanase treatment)	Irregular	60 to 120	(Sun et al., 2014)
Corn starch	Enzymatic (Amylase) hydrolysis of starch –butanol complex	Sphere or oval	10 to 20	(Kim & Lim, 2009)
Maize, potato and cassava starches	Enzymolysis (Amylase treatment)	Spherical, Octahedral, Spherical, respectively.	162 ± 23, 301 ± 90, 255 ± 61, respectively.	Present study

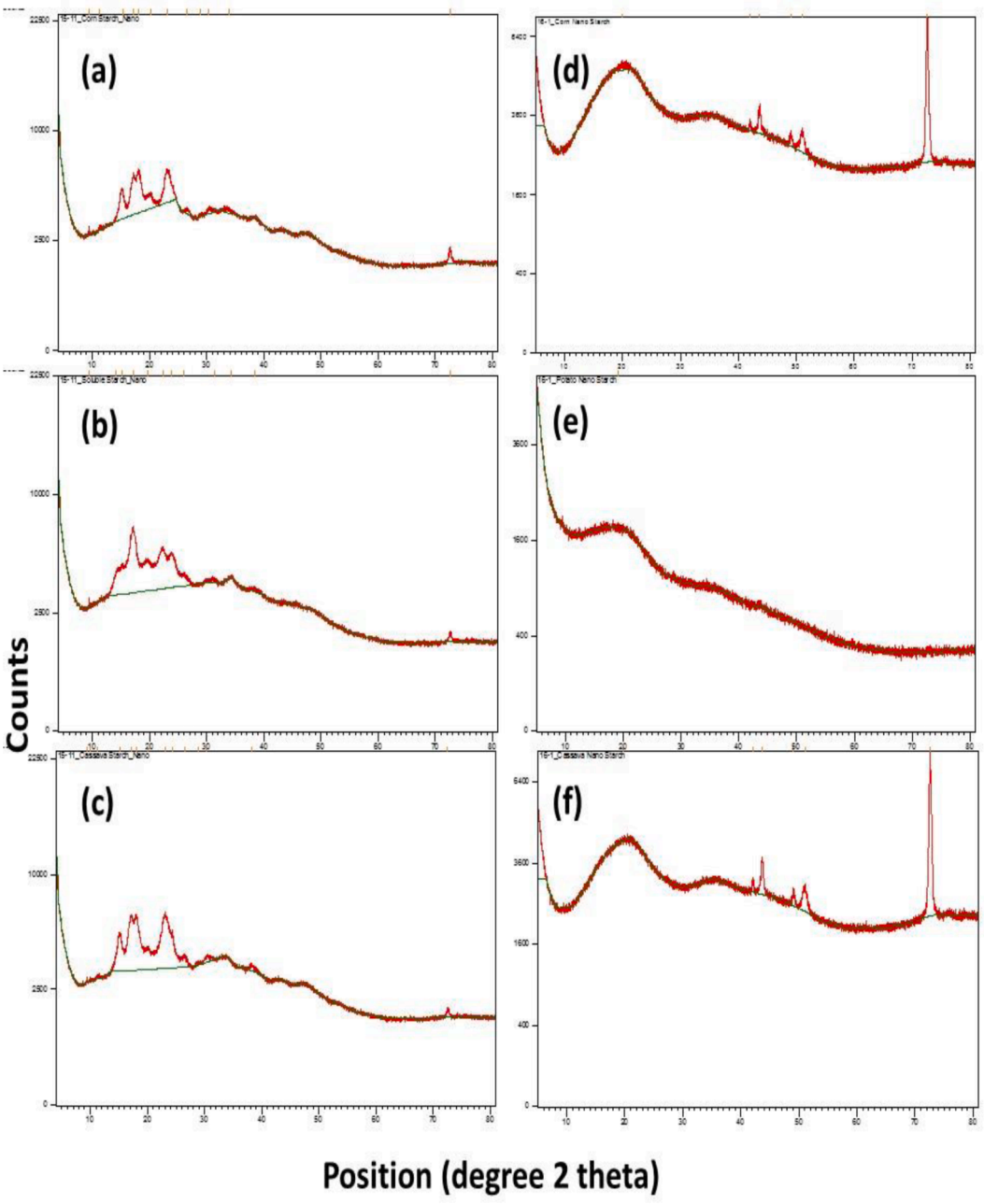

Fig. 3. XRD spectra of native starch from maize (a), potato (b) and cassava (c) and enzyme hydrolyzed nanostarch from maize (d), potato (e) and cassava (f).

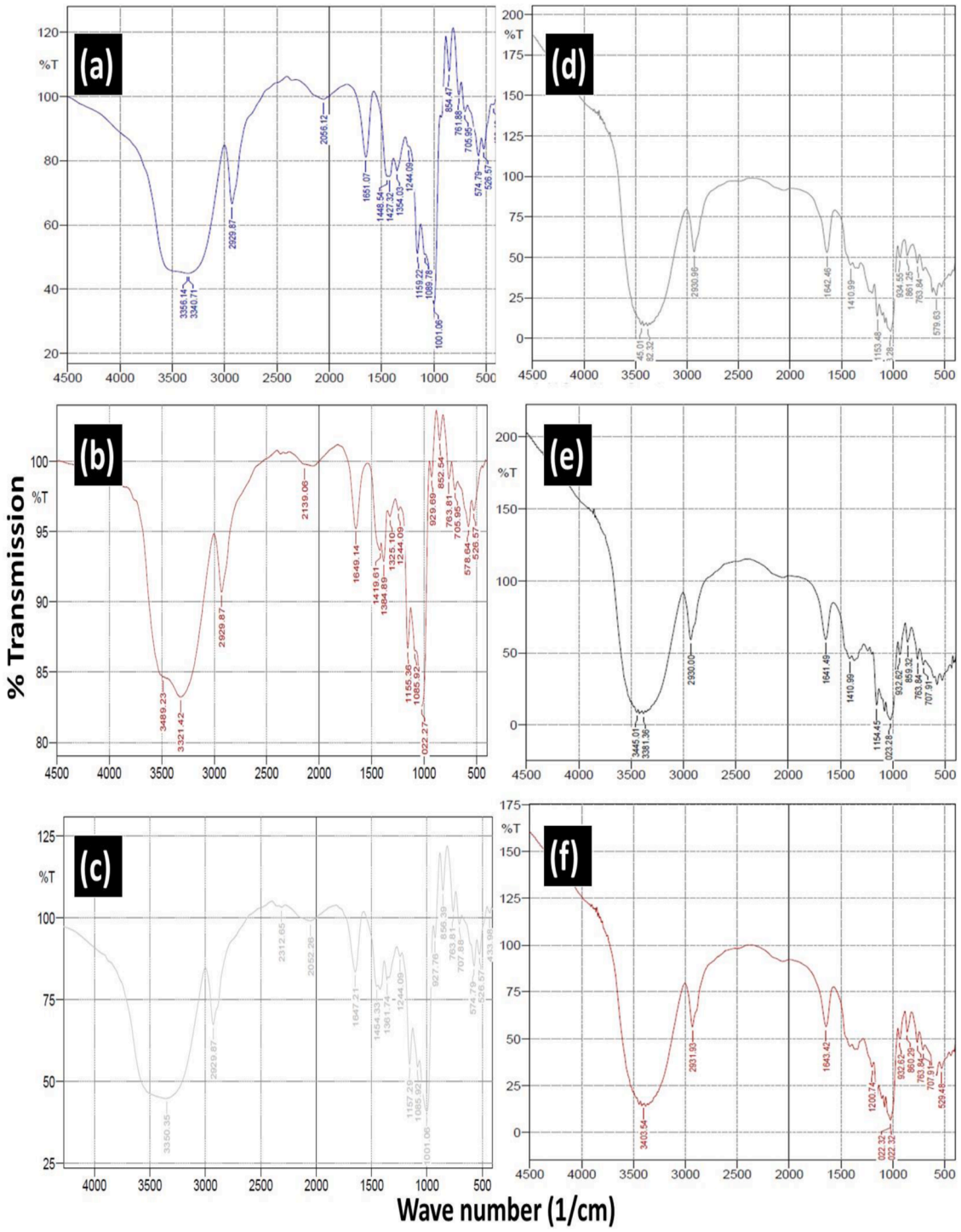

Fig. 4. FTIR spectra of native starch from maize (a), potato (b) and cassava (c) and enzyme hydrolyzed nanostarch from maize (d), potato (e) and cassava (f).

work, a maximum yield of 41% and 35% could be achieved by enzyme and acid hydrolyses, respectively.

The SEM images of acid hydrolyzed and enzyme hydrolyzed nanostarches are given in Fig. 1. The nanostarches obtained from maize by both acid (Fig. 1a) and enzyme (Fig. 1d) hydrolysis resulted in ultrafine sized (less than 50 nm) spherical nanoparticles. In the case of potatoes, the resultant nanostarches by acid hydrolysis (Fig. 1b) and enzyme (Fig. 1e) assisted processes were octahedral shaped and in the size range of about 300 nm. Also, many of the particles looked aggregated that could have happened during the drying process. In the case of cassava, the acid process resulted in an octahedral shape (Fig. 1c) and the enzyme process resulted in a spherical shape (Fig. 1f); and, the sizes were in the range of 300 to 400 nm. The size observed in SEM images did not match well with that of DLS analysis since no cross-linkers or stabilizers were used, resulting in aggregation during the drying of samples.

Fig. 2 shows the TEM micrographs of the nanostarches stained using uranyl acetate. The average sizes obtained by image analyses are given in table 2. While the acid hydrolyzed nanostarches are well below 100 nm size, the enzymatic process resulted in the size ranging between 100 to 300 nm and also with wide size distribution. The morphology / shape of the observed nanostarches were in line with that of SEM observations. Here, aggregations were not prominent possibly due to the addition of

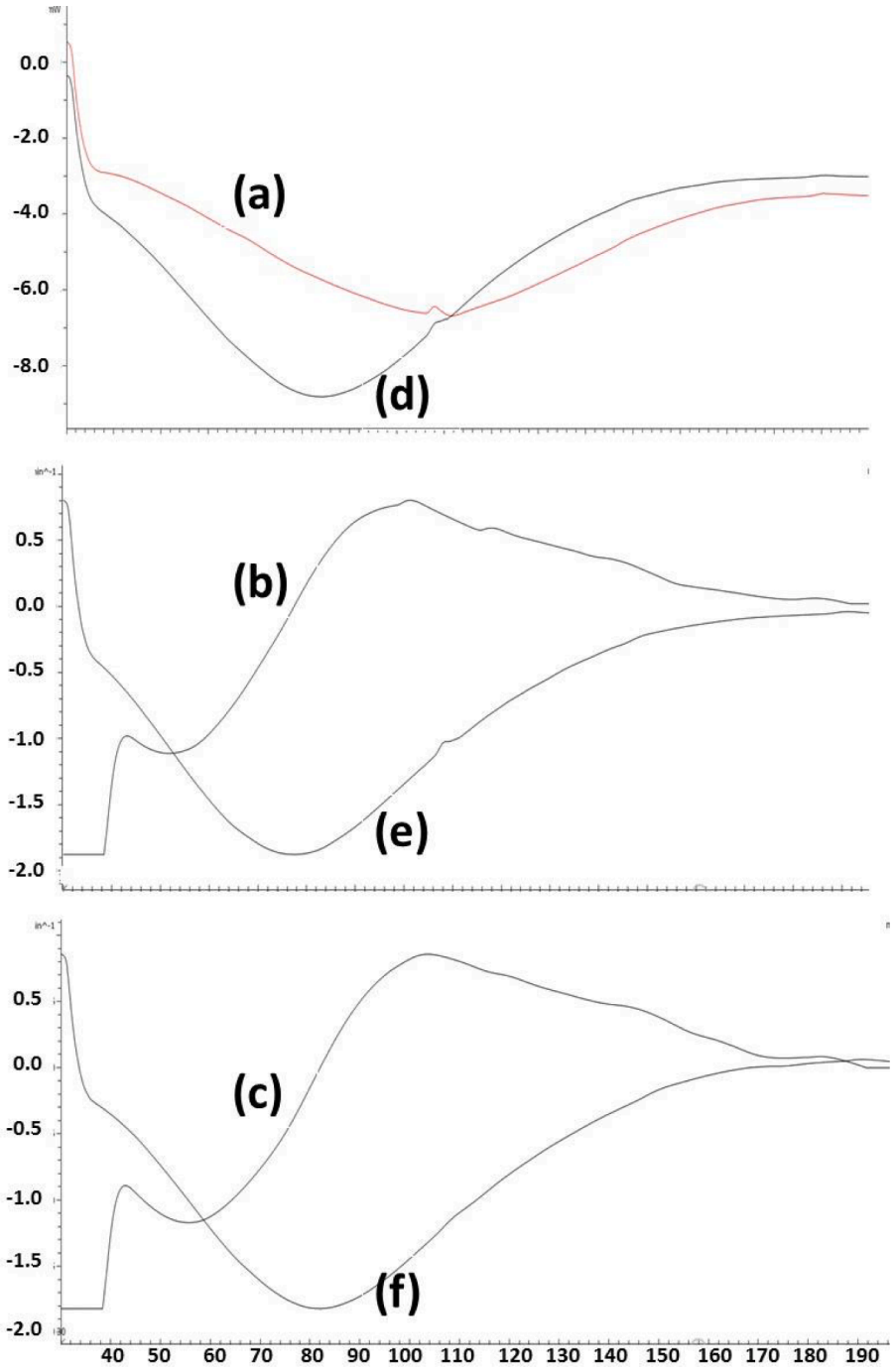

Fig. 5. DSC spectra of hydrolyzed nanostarch from maize (a), potato (b) and cassava (c) and native starches from maize (d), potato (e) and cassava (f).

uranyl acetate during the drying process. Though the mechanical process (homogenization followed by extrusion) is easily scalable for nanostarch production, it is difficult to achieve a size range of less than 100 nm (Chen et al., 2018). Hence, a process like acid hydrolysis is crucial in achieving a size much lesser than 100 nm, as demonstrated in this work. But, enzyme hydrolysis could not achieve the desired size range, may be due to the comparatively larger size of the enzyme molecules (than that of acid molecules) that attack the starch polymer.

Table 3 lists the recent studies reporting the enzymatic preparation of nanostarches and their relevant characteristics. From this table, it is clear that chemical treatment coupled with the enzymatic hydrolysis/catalyzed reactions have resulted in the production of starch nanoparticles with reduced size. In this work, we have produced nanostarches using enzyme treatment alone. Consequently, the size of obtained nanostarches was comparatively higher than that of the literature values. In regards to the morphology, we have almost obtained similar shapes of different nanostarches prepared using the enzyme hydrolysis approach for maize and cassava. Only in case of potato starch, we have obtained an octahedral shape of nanostarch and such a shape was not reported earlier. Hence, the source of starch biopolymers influences the shape of the resulting nanostarch. Based on the size and shape requirement of intended application, we need to choose the source of the starch and also the method of hydrolysis.

In XRD analysis, all the starches exhibited diffraction peaks around 15, 18 and 23 degrees indicating the presence of A-type crystal arrangement (Fig. 3). The hydrolysis with α-amylase changed the X-ray

pattern significantly in all three starches and substantially decreased the crystalline components. The relative crystallinity of native starches, 34.5, 31.2 and 29.4 were reduced to 21.3, 17.5 and 13.2 in maize, potato and cassava nanostarches, respectively. This indicates that the hydrolysis by α-amylase eroded not only the amorphous region but also, significantly eroded the crystalline region. A similar reduction in crystallinity was reported earlier, during 24 h of hydrolysis (Kim et al., 2008). In the case of acid hydrolysis, the amorphous region is preferentially attacked, thereby retaining more amount of the crystalline region. Earlier work reported the nanostarch exhibiting typical V-type crystalline structures that were independent of the crystal type of the native starch and the relative crystallinity of nanostarch increased with the increasing amylose content in native starch (Qin et al., 2016).

The FTIR spectra of nanostarches are given in Fig. 4 and the characteristic bands correspond to the vibrational modes of amylose and amylopectin components of starch. The strong absorption band in the range of 3500–3300 cm^{-1} was attributed to the O–H stretching of starch. The C-H stretching peak was observed at around 2930 cm^{-1} in all the samples. The absorption bands that appeared in between 1000 cm^{-1} and 1200 cm^{-1} were characteristic of the C–O stretching of the polysaccharide skeleton. The bands between 850 to 860 cm^{-1} were sensitive to crystallinity changes (Sun et al., 2014). This peak in all nanostarch samples shifted towards higher wave numbers, to the level of 5 to 10 cm^{-1}. The peak expected at 960 cm^{-1} to represent the skeletal mode vibrations of α-1,4glycosidic linkage (C–O–C), and the peak of the C–O–C group of all the nanostarch samples were shifted toward lower wave numbers to around 932 cm^{-1} indicating that the hydrogen bonds between starch molecular chains in the nanostarch were stronger compared to their native counterparts.

Fig. 5 shows the DSC thermograms of the native starch and their hydrolyzed nanostarch counterparts. The increase in melting enthalpy after enzyme hydrolysis suggested the preferential erosion of amorphous region of starch, in line with the observation of XRD analysis. Also, it affected the melting of crystals as water became more readily accessible to the crystalline regions after the erosion of amorphous region. The endotherm peaks of gelatinization for native starches were observed at 84°C, 78°C and 82°C for maize, potato and cassava, respectively. These peaks shifted to 52°C and 56°C, respectively in case of nanostarches of potato and cassava. In case of maize nanostarch, this peak shifted well below 50°C. A similar result was reported earlier wherein, the gelatinization enthalpy of the corresponding nanostarch decreased when compared with native starch, except for high amylose maize starch (Qin et al., 2016). An earlier work reported that the ultrasound-processed nanostarch was more similar to native starch; while that prepared by acid hydrolysis showed the greatest difference, being more soluble, more translucent and more hygroscopic (Gonçalves et al., 2014).This work compared the nanostarches prepared by acid and enzyme hydrolyses and established the differences among the nanostarches prepared from maize, potato and cassava starches..

4. Conclusions

Nanostarch, originated from biopolymer, has the potential for applications in biocomposites, food and pharmaceutical areas. Traditionally, the protocols developed for the production of nanostarch focused on acid hydrolysis, ultrasonication, homogenization and precipitation. This work focused on the development of an enzymatic process for the production of nanostarches from maize, potato and cassava starches. The acid hydrolysis resulted in a much smaller size of nanostarch as compared to that of enzyme hydrolysis. The nanostarch produced from maize is smaller than that of potato and cassava. An enzymatically prepared nanostarch was found to aggregate during the drying process as observed in SEM, since cross-linkers/stabilizers were not added during the process. The hydrogen bonds between the molecular chains in nanostarch were stronger compared to their native counterparts as analyzed by FTIR. The melting enthalpies of nanostarches were lower than their bulk counterparts. Though the size of enzyme processed nanostarch is bigger than that of the acid process, the eco-friendly enzymatic process will add to its value for diversified applications.

Declaration of Competing Interest

The authors declare that they have no known competing financial interests or personal relationships that could have appeared to influence the work reported in this paper.

Acknowledgments

First author is highly thankful to the Director, ICAR-CIPHET, Ludhiana (Punjab) for allowing his professional attachment training at ICAR-CIRCOT, Mumbai. Authors also thank Dr. N.M. Ashtaputre, Dr. Charlene D' Souza, Mr. Manoj Ambare, Mrs. Sujata Kawlekar, Mr. Nishant Kambli and Mr. Rajesh P Kadam of ICAR-Central Institute for Research on Cotton Technology, Mumbai, India for their technical support to carry out this research work.

References

Acevedo-Guevara, L., Nieto-Suaza, L., Sanchez, L. T., Pinzon, M. I., & Villa, C. C. (2018). Development of native and modified banana starch nanoparticles as vehicles for curcumin. *International Journal of Biological Macromolecules, 111*, 498–504.

Apostolidis, E., & Mandala, I. (2020). Modification of resistant starch nanoparticles using high-pressure homogenization treatment. *Food Hydrocolloids, 103*, Article 105677.

Angellier, H., Choisnard, L., Molina-Boisseau, S., Ozil, P., & Dufresne, A. (2004). Optimization of the Preparation of Aqueous Suspensions of Waxy Maize Starch Nanocrystals Using a Response Surface Methodology. *Biomacromolecules, 5*(4), 1545–1551.

Chang, R., Ji, N., Li, M., Qiu, L., Sun, C., Bian, X., Qiu, H., Xiong, L., & Sun, Q. (2019). Green preparation and characterization of starch nanoparticles using a vacuum cold plasma process combined with ultrasonication treatment. *Ultrasonics Sonochemistry, 58*, Article 104660.

Chen, Q., Dong, X., Zhou, L., Zheng, X., Wang, J., & Wang, P. (2018). Nanostarch surface coating of lightweight coated paper. *BioResources, 13*(1), 729–739.

Chena Aldao, D., Šárka, E., Ulbrich, P., & Menšíková, E. (2018). Starch nanoparticles–two ways of their preparation. *Czech Journal of Food Science, 36*, 133–138.

Chin, S. F., Mohd Yazid, S. N. A., & Pang, S. C. (2014). Preparation and characterization of starch nanoparticles for controlled release of curcumin. *International Journal of Polymer Science, 2014*, 8. https://doi.org/10.1155/2014/340121.

Condés, M. C., Añón, M. C., Mauri, A. N., & Dufresne, A. (2015). Amaranth protein films reinforced with maize starch nanocrystals. *Food Hydrocolloids, 47*, 146–157.

Cuthbert, W. O., Ray, S. S., & Emmambux, N. M. (2017). Isolation and characterization of nanoparticles from tef and maize starch modified with stearic acid. *Carbohydrate Polymers, 168*, 86–93.

Dong, H., Zhang, Q., Gao, J., Chen, L., & Vasanthan, T. (2021). Comparison of morphology and rheology of starch nanoparticles prepared from pulse and cereal starches by rapid antisolvent nanoprecipitation. *Food Hydrocolloids, 119*, Article 106828. https://doi.org/10.1016/j.foodhyd.2021.106828.

DuBois, M., Gilles, K. A., Hamilton, J. K., Rebers, P. A., & Smith, F. (1956). Colorimetric Method for Determination of Sugars and Related Substances. *Analytical Chemistry, 28*(3), 350–356.

Dufresne, A. (2015). Starch and nanoparticle. In: K. G., Ramawat & J. M., Mérillon (Eds). *Polysaccharides: Bioactivity and biotechnology* (pp. 417–449). Cham: Springer International Publishing.

El-Naggar, M. E., El-Rafie, M. H., El-sheikh, M. A., El-Feky, G. S., & Hebeish, A. (2015). Synthesis, characterization, release kinetics and toxicity profile of drug-loaded starch nanoparticles. *International Journal of Biological Macromolecules, 81*, 718–729.

Gonçalves, P. M., Noreña, C. P. Z., da Silveira, N. P., & Brandelli, A. (2014). Characterization of starch nanoparticles obtained from *Araucaria angustifolia* seeds by acid hydrolysis and ultrasound. In *LWT-Food Science and Technology, 58* pp. 21–27).

Hao, Y., Chen, Y., Lia, Q., & Gao, Q. (2018). Preparation of starch nanocrystals through enzymatic pretreatment from waxy potato starch. *Carbohydrate Polymers, 184*, 171–177.

Kim, H. Y., Park, S. S., & Lim, S. T. (2015). Preparation, characterization and utilization of starch nanoparticles. *Colloids and surfaces B, Biointerfaces, 126*, 607–620.

Kim, J. Y., & Lim, S. T. (2009). Preparation of nano-sized starch particles by complex formation with n-butanol. *Carbohydrate Polymers, 76*(1), 110–116.

Kim, J. Y., Park, D. J., & Lim, S. T. (2008). Fragmentation of waxy rice starch granules by enzymatic hydrolysis. *Cereal Chemistry Journal, 85*(2), 182–187.

Kumar, S., Verma, S., & Jain, S. L. (2015). Base-free direct formylation of aromatic iodides using CO_2 as C_1 source catalyzed by palladium nanoparticles grafted onto amino-functionalized nanostarch. *Tetrahedron Letters, 56*(19), 2430–2433.

Le Corre, D., & Angellier-Coussy, H. (2014). Preparation and application of starch nanoparticles for nanocomposites: A review. *Reactive and Functional Polymers, 85*, 97–120.

Le Corre, D., Bras, J., & Dufresne, A. (2010). Starch nanoparticles: A review. *Biomacromolecules, 11*(5), 1139–1153.

Lin, N., Huang, J., Chang, P. R., Anderson, D. P., & Yu, J. (2011). Preparation, modification, and application of starch nanocrystals in nanomaterials: A review. *Journal of Nanomaterials*, 13, 2011.

Liu, Q., Cai, W., Zhen, T., Ji, N., Dai, L., Xiong, L., & Sun, Q. (2020). Preparation of debranched starch nanoparticles by ionic gelation for encapsulation of epigallocatechin gallate. *International Journal of Biological Macromolecules, 161*, 481–491.

Maleki, A., Eskandarpour, V., Rahimi, J., & Hamidi, N. (2019). Cellulose matrix embedded copper decorated magnetic bionanocomposite as a green catalyst in the synthesis of dihydropyridines and polyhydroquinolines. *Carbohydrate Polymers, 208*, 251–260.

Maleki, A., Movahed, H., & Ravaghi, P. (2017). Magnetic cellulose/Ag as a novel eco-friendly nanobiocomposite to catalyze synthesis of chromene-linked nicotinonitriles. *Carbohydrate Polymers, 156*, 259–267.

Md. Sharif, H., Itaru, S., Makiko, T., Seiichiro, I., Mitsutoshi, N., & Hiroshi, O. (2011). Effect of Particle Size of Difference Crop Starches and Their Flours on Pasting Properties. *Japan Journal of Food Engineering, 12*(1), 29–35.

Patel, C. M., Chakraborty, M., & Murthy, Z. V. P. (2016). Fast and scalable preparation of starch nanoparticles by stirred media milling. *Advanced Powder Technology, 27*(4), 1287–1294.

Putro, J. N., Ismadji, S., Gunarto, C., Soetaredjo, F. E., & Ju, Y. H. (2020). A study of anionic, cationic, and nonionic surfactants modified starch nanoparticles for hydrophobic drug loading and release. *Journal of Molecular Liquids, 298*, Article 112034.

Qi, X., & Tester, R. F. (2016). Effect of native starch granule size on susceptibility to amylase hydrolysis. *Starch –Stärke, 68*(9-10), 807–810.

Qin, Y., Liu, C., Jiang, S., Xiong, L., & Sun, Q. (2016). Characterization of starch nanoparticles prepared by nanoprecipitation: Influence of amylose content and starch type. *Industrial Crops and Products, 87*, 182–190.

Rajisha, K. R., Maria, H. J., Pothan, L. A., Ahmad, Z., & Thomas, S. (2014). Preparation and characterization of potato starch nanocrystal reinforced natural rubber nanocomposites. *International Journal of Biological Macromolecules, 67*, 147–153.

Repo-Carrasco-Valencia, R., Acevedo de La Cruz, A., Icochea Alvarez, J. C., & Kallio, H. (2009). Chemical and Functional Characterization of Kañiwa (*Chenopodium pallidicaule*) Grain, Extrudate and Bran. *Plant Foods for Human Nutrition, 64*(2), 94–101.

Roy Goswami, S., Dumont, M. J., & Raghavan, V. (2016). Starch to value added biochemicals. *Starch - Stärke, 68*(3-4), 274–286.

Shabana, S., Prasansha, R., Kalinina, I., Potoroko, I., Bagale, U., & Shirish, S. H. (2019). Ultrasound assisted acid hydrolyzed structure modification and loading of antioxidants on potato starch nanoparticles. *Ultrasonics Sonochemistry, 51*, 444–450.

Sun, Q., Gong, M., Li, Y., & Xiong, L. (2014). Effect of retrogradation time on preparation and characterization of proso millet starch nanoparticles. *Carbohydrate Polymers, 111*, 133–138.

Yu, M., Ji, N., Wang, Y., Dai, L., Xiong, L., & Sun, Q. (2021). Starch-based nanoparticles: Stimuli responsiveness, toxicity, and interactions with food components. *Comprehensive Reviews Food Science and Food Safety, 20*, 1075–1100. https://doi.org/10.1111/1541-4337.12677.

Verma, S., Le Bras, J., Jain, S. L., & Muzart, J. (2013). Thiol-yne click on nano-starch: An expedient approach for grafting of oxo-vanadium Schiff base catalyst and its use in the oxidation of alcohols. *Applied Catalysis A: General, 468*, 334–340.

Waterschoot, J., Gomand, S. V., Fierens, E., & Delcour, J. A. (2015). Production, structure, physicochemical and functional properties of maize, cassava, wheat, potato and rice starches. *Starch – Stärke, 67*(1-2), 14–29.

Xie, F., Pollet, E., Halley, P. J., & Avérous, L. (2013). Starch-based nano-biocomposites. *Progress in Polymer Science, 38*(10), 1590–1628.

Zoveidavianpoor, M., & Samsuri, A. (2016). The use of nano-sized Tapioca starch as a natural water-soluble polymer for filtration control in water-based drilling muds. *Journal of Natural Gas Science and Engineering, 34*, 832–840.